

Inverter transient response improvement using grey wolf optimizer for type-2 fuzzy control in HVDC transmission link

I Made Ginarsa¹, Agung Budi Muljono¹, I Made Ari Nrartha¹, Ni Made Seniari¹, Sultan¹, Osea Zebua²

¹Department of Electrical Engineering, Faculty of Engineering, University of Mataram, Mataram, Indonesia

²Department of Electrical Engineering, Faculty of Engineering, University of Lampung, Bandar Lampung, Indonesia

Article Info

Article history:

Received Dec 20, 2024

Revised Jun 6, 2025

Accepted Jul 23, 2025

Keywords:

Grey wolf optimizer

High voltage direct current

Inverter controller

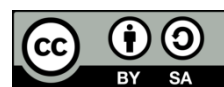
Transient response maintain

Type-2 fuzzy

ABSTRACT

High voltage direct current (HVDC) on transmission-link becomes a new prominent technology in recent years. The HVDC is applied to transmit amount of electrical energy from power plant to consumers. This method makes reactive power losses on transmission devices decrease significantly and stability level of generator increases. However, inverter HVDC transmission system can produce slow and high inverter transient current (ITC) response at high value of the up-ramp rate. This ITC phenomenon can be serious problem at starting time. So grey wolf algorithm is proposed to optimize input-output parameters of interval type-2 fuzzy control (IT2FC) in inverter-side HVDC. The proposed control performance's is assessed by integral time squared error (ITSE) and peak overshoot (M_p) approaches. Simulation results show that small ITSE and low M_p of transient response are given by the IT2FC. The IT2FC is successful applied on inverter HVDC with better results compared to conventional PI control scheme.

This is an open access article under the [CC BY-SA](https://creativecommons.org/licenses/by-sa/4.0/) license.



Corresponding Author:

I Made Ginarsa

Department of Electrical Engineering, Faculty of Engineering, University of Mataram

Majapahit St., No. 62 Mataram, NTB 63125, Indonesia

Email: kadekgin@unram.ac.id

1. INTRODUCTION

Modern power industries consist of power plant, transmission line, distribution and load systems. The transmission system function is to transfer amount of the electric energy from power generation plants (fossil or renewable energy sources) to distribution systems, moreover to consumers. There are two transmission types exist such as: alternating current (AC) and direct current (DC). By implementing modern power semiconductor and its controller technologies, the power convert from AC to DC or vice-versa is easy to be implemented in real power system (PS) with affordable cost. The electrical power is transferred into high voltage direct current (HVDC) formed, furthermore the power is transmitted to consumers in demand side. Some advantages of HVDC transmission line such as: Can be installed on far distance by overhead or/and sea cables, reactive power losses can be reduced, can be connected with all power systems frequency in the worldwide, to minimize angle stability problem in longer transmission line distance, and can be operated with higher reliability. Those advantages make the HVDC link more competent to transmit the electrical power than high voltage alternating current (HVAC) transmission system [1]. It is not only to deliver the electrical power in the traditional sense, but also cooperate with smart mobile communication devices, internet, internet of thing, and has applied widely in recent years [2]. Meanwhile, a voltage source converter (VSC) HVDC is developed to deliver a large scale of electrical power from renewable energy source generation to the bulk of modern PS operations. The Kriging surrogate method is built for configuration model optimization of reactive power compensator to maintain the power transfer using a bi-level optimal power flow algorithm [3]. Moreover, ultra HVDC (UHVDC) transmission system is a new technology can be used to gain the power

transfer, to minimize the losses, and to reduce circuit-line number [4]. The structure and characteristic operations of UHVDC are analyzed with two indices such that partial mono-pole and bi-pole outage times [5]. Simplified model HVDC is developed to reduce complicated of HVDC model and to reduce simulation time [6]. To protect and isolate the HVDC circuit when the fault occurred on the HVDC circuit, the integrated HVDC circuit breaker with past enough to clear the DC fault is proposed [7]. Frequency limit control is applied to improve frequency stability in islanded HVDC system and avoid frequency deviation significantly [8]. Modeling and analysis a regulation scheme real time for frequency both converter and inverter are proposed to gain power capacity and to enhance transient period for short-term-transferred on line-commutated converter (LCC) of HVDC [9], [10]. The features of panoramic voltage and vision transformers are implemented for location of fault accurately in high voltage direct-current grids [11].

The HVDC structure for linear analysis and small signal modeling (SSM) are built to reduce model complexity and to maintain the accuracy of the SSM in low-frequency oscillation [12], transfer function matrix-based SSM with time-frequency analysis is proposed to maintain quantitative stability and dynamic performance of multi-terminal HVDC considering different operation mode [13]. The SSM model is applied to stability analysis on different HVDC station topologies in asymmetric direct-current mode operations with grounding HVDC network consideration and to build controller for improvement of system response during asymmetric DC operation [14]. Supervisory control is applied in HVDC that allows the controller to be separated into three levels of detail function such as: Supervision, logic and interface level controls [15]. Optimal operation of HVDC-HVAC is executed by AC/DC optimal power flow appropriate voltage reference to the grid side converter's control periodically and the system can still be operated even during contingencies such as on converter or DC cable disconnection [16]. Optimal control scheme for HVDC to improve robust grid frequency regulation [17], hybrid VSC/LCC cascaded HVDC is developed to support reactive power maintain in large capacity transfer [18], and fast protection scheme is proposed based on un-distorted factor using line traveling wave voltage to obtain the detailed protection criteria [19]. Development of artificial intelligent (AI) and its applications penetrate into electrical engineering field such as: Adaptive neuro-fuzzy inference system (ANFIS)-based passivity control is used in multilevel inverter [20], in supplementary control for reduce transient current on rectifier [21] and in HVDC system to reduce transient current of rectifier [22].

Generally, optimization algorithm (OA) is built in mathematical and meta-heuristic models [23]. The meta-heuristic algorithm is divided into four categories [24]: (a). Genetic algorithms. Evolutionary genetic evolution in biology is inspired this algorithm. Reproduction, mutation, recombination, and selection processes should be done in this algorithm. For example, tree growth algorithm is developed on the evolutionary principal. (b). Swarm intelligence. This algorithm mimics the animal habit of food foraging or schooling. Giant trevally optimizer is included in this category, and this algorithm is applied in engineering system. Meanwhile, grey wolf optimizer (GWO) is designed on shape and size 800-kV converter transformer bushing optimization for HVDC system [25]. (c). Human activity algorithm. This algorithm imitates the human activities in process of preschool education [26] or interaction of teaching-learning for teacher-pupil in classroom. This method is applied on grid-connected photovoltaic-battery system [27]. (d). The OAs are built from other inspiration, such as optimization inspired from crystal structure algorithm to imitate the crystal formation in symmetric arrangement in nature [28], material generation and formation in natural environment [29], application of gravitational search algorithm for automatic load frequency control on hybrid PS(s) [30].

Transient response in HVDC system should paid attention in order to maintain short-term power transfer [10]. Nevertheless, IT2FC-GWO research topic in reducing transient response in an inverter HVDC system has not been treated in the previous literatures. To use this control scheme, The IT2FC optimized by the GWO to enhance the ITC response in inverter-side HVDC is implemented. The rest of the manuscript is managed as following: The HVDC structure and IT2FC scheme are explored in Section 2. Section 3, develop and adjust the GWO parameters. The results of simulation in numeric value, graphic and table forms and their explanations are provided in Section 4. Finally, Section 5 shows the summary of this research.

2. HVDC TRANSMISSION LINE CONTROLLED BY TYPE-2 FUZZY SYSTEM

2.1. HVDC system

Delivering amount of electric energy from power plant production to loading side is the main function of HVDC transmission line. In this research, the model and its operation procedure are developed by [31], where the numbering in parentheses refers to the block components shown in Figure 1:

- | | |
|---|--|
| 1) Sending-end from rectifier | 5) Transducer for inverter measurement |
| 2) A three hundred kilometers long-distance DC-line | 6) A receiving-end voltage source |
| 3) RL compensator | 7) A 600 MVAR 50 Hz AC filter |
| 4) Inverter device | |

To run the inverter HVDC this system components:

- | | |
|---|--|
| 20) Master control | 23) PI control |
| 5) Signal inputs V_{abc}, I_{abc} from transducer | 24) IT2FC-GWO |
| 21) I_{eff} calculation | 25) Inverter pole control), and generate pulse |
| 22) Current error calculation (Ei) | inverter ignition in 12-pulse firing control |

The PI control is modified by adding an (IT2FC-GWO) as a supplementary controller. The numbering in parentheses below refers to the sub-components depicted in Figure 1(b):

- | | |
|---------------------|---|
| 24a) Input | 24e) Interval type-2 fuzzy model |
| 24b) Gain K_{in1} | 24f) Gain for K_{out} |
| 24c) Gain K_{in2} | 24g) GWO algorithm |
| 24d) Unit delay | 24h) Alpha (α_i) signal as an output |

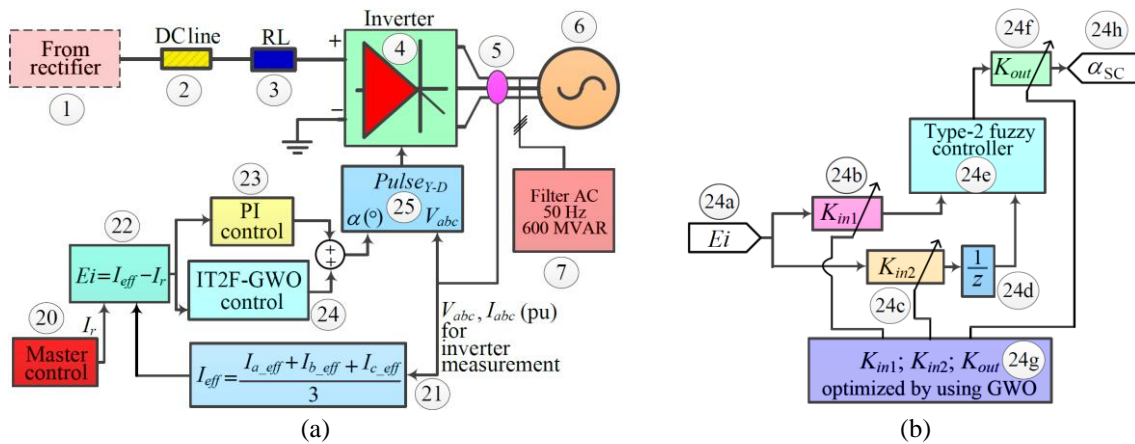


Figure 1. Inverter HVDC diagram: (a) main apparatus and (b) IT2FC-GWO proposed control

2.2. Interval type-2 fuzzy control (IT2FC)

The IT2FC was developed by five Gaussian membership (MF) functions on two inputs and nine constant-type MFs on an output. The MF function for Input dEi and nine constant-type MFs for the Output are illustrated in Figures 2(a) and 2(b), respectively. The constant values of respective output MFs are:

- | | | |
|-------------|-------------|------------|
| MF1 = -1 | MF4 = -0.25 | MF7 = 0.5 |
| MF2 = -0.75 | MF5 = 0 | MF8 = 0.75 |
| MF3 = -0.5 | MF6 = 0.25 | MF9 = 1 |

Nine fuzzy rules (Rule 1 – Rule 9) were built to generate an output based on the evaluation of Input Ei and dEi , as shown in Figure 2(c). Each rule is expressed in linguistic terms, as defined in (1). The rule base includes the following linguistic variables:

- | | |
|---------------------------|---------------------------|
| NBU: Negative big upper | ZEL: Zero lower |
| NBL: Negative big lower | PSU: Positive small upper |
| NSU: Negative small upper | PSL: Positive small lower |
| NSL: Negative small lower | PBU: Positive big upper |
| ZEU: Zero upper | PBL: Positive small lower |

Example for Rule 7: If (Ei is PBU, Positive Big Upper) and (dEi is PSU, Positive Small Upper), Then SC is MF7. Furthermore, the input and output connection defined as input-output surface-control as shown in Figure 2(d).

- | | | |
|------|---|-----|
| Rule | 1: If (Ei is NBU) and (dEi is NBU) Then (SC is MF1) | |
| | 2: If (Ei is NSU) and (dEi is NBU) Then (SC is MF2) | |
| | 3: If (Ei is NBU) and (dEi is NSU) Then (SC is MF3) | |
| | 4: If (Ei is NSU) and (dEi is NSU) Then (SC is MF4) | |
| | 5: If (Ei is ZEU) and (dEi is ZEU) Then (SC is MF5) | |
| | 6: If (Ei is PSU) and (dEi is PSU) Then (SC is MF6) | |
| | 7: If (Ei is PBU) and (dEi is PSU) Then (SC is MF7) | |
| | 8: If (Ei is PSU) and (dEi is PBU) Then (SC is MF8) | |
| | 9: If (Ei is PBU) and (dEi is PBU) Then (SC is MF9) | (1) |

2.3. Development of fitness function

On start mode the master control generates current reference signal (I_r), this signal is used to guide the PI and IT2FC-GWO controls to ignite pole angle signal (αi). Next, this signal is used to fire PWM (12-pulse firing control) for arms Y and D of inverter. Current error signal (difference between current effective signal (I_{eff}) and current reference, I_r) is used as the feedback signal for control signal. Calculation of error signal is formulated in (2). The main rule of the controller is to minimize the current error signal during the starting mode. Current effective is computed using (3). Figure 3 show the current effective response of 3-phase HVDC inverter and current reference. The fitness function (F_{fit}) is built follow the idea on [32] using (4).

$$Ei = I_{eff} - I_r \quad (2)$$

$$I_{eff} = \frac{1}{3} (I_{a_eff} + I_{b_eff} + I_{c_eff}) \quad (3)$$

$$F_{fit} = \int_{t_1}^{t_6} t \times (Ei)^2 dt \quad (4)$$

Where Ei is the current error signal, I_{a_eff} , I_{b_eff} , I_{c_eff} are the current effective signal of phase A, B, C, and t is time from t_1 to t_6 .

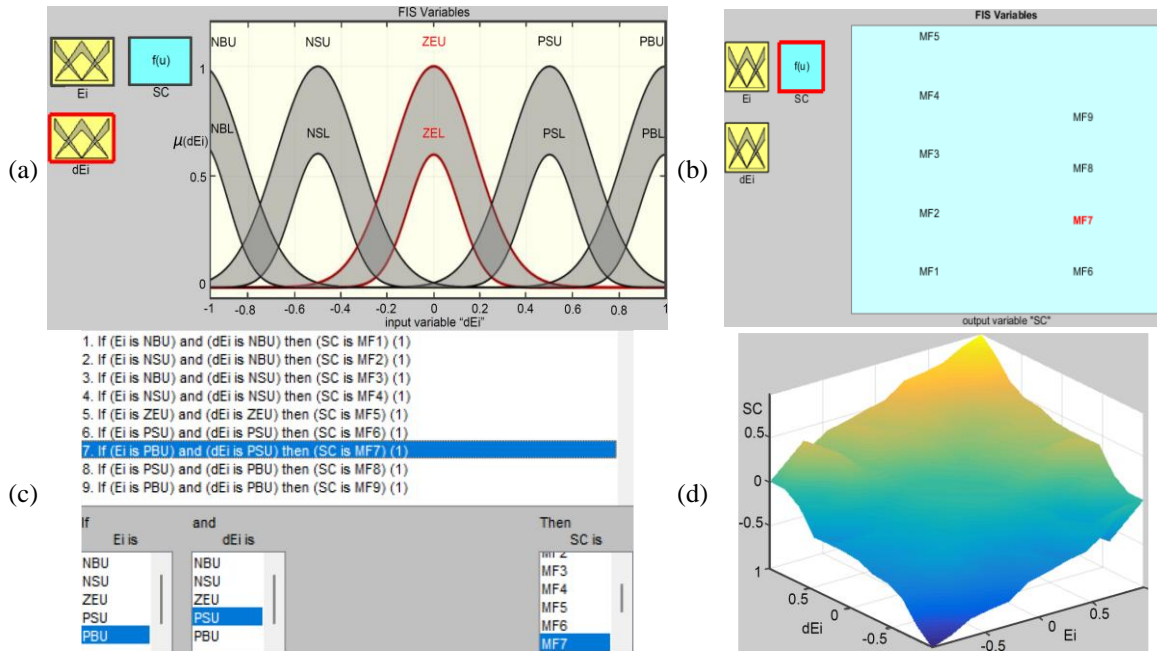


Figure 2. IT2FC model: (a) input MF, (b) output MF, (c) rule base, and (d) surface control of the IT2FC

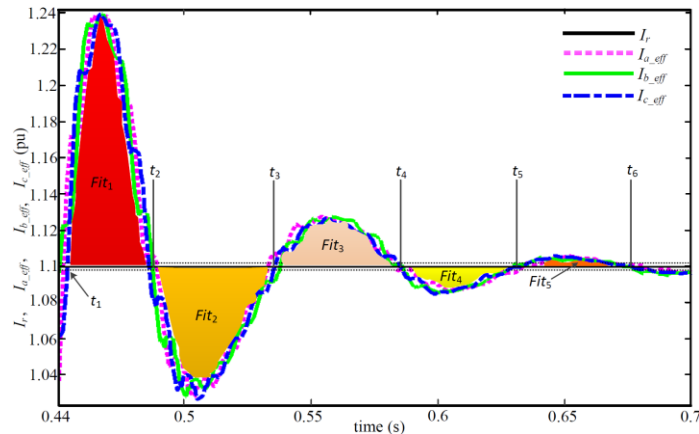


Figure 3. Built of fitness function for phase current ABC and reference current

3. GREY WOLF OPTIMIZER (GWO) METHOD

A unique behavior of grey wolves pack (as predator) to hunt and search prey in natural wild is named grey wolf optimizer (GWO) model in [33]. This meta-heuristic population-based optimization has good convergence ability toward the optima and has the ability to avoid the local optima stagnation. The leadership and hierarchy procedures are very strong in social life of the wolf packs. This GWO has four levels social hierarchy such as: α (alpha) for first level, β (beta) for second level, δ (delta) for third level and ω (omega) for last level.

3.1. Social live and hunting in wild nature

The beta wolf is the best candidate to be the alpha, takes from other wolves and give it to the alpha leader. Next, the third level of the grey wolves is beta wolves, these wolves dominate of the forth level. The last level is named omega wolves, which are responsible for maintaining the safety and integrity in the wolf pack. When the grey wolf found the candidate prey, they will reach by encircling the prey immediately. Mathematical model to illustrate the stage is formulated by (5) and (6).

$$\bar{D} = |\bar{C} \cdot \bar{X}_{py}(iter) - \bar{X}_g(iter)| \quad (5)$$

$$\bar{X}_g(iter + 1) = \bar{X}_{py}(iter) - \bar{A} \cdot \bar{D} \quad (6)$$

Where $iter$, (\bar{A} and \bar{C}), \bar{X}_{py} and \bar{X}_g are the current iteration, vector coefficient, prey and grey wolf position vectors, respectively. Furthermore, the (6) and (7) are used to computed the vectors \bar{A} and \bar{C} .

$$\bar{A} = 2 \cdot \bar{a} \cdot \bar{r}_1 - \bar{a} \quad (7)$$

$$\bar{C} = 2 \cdot \bar{r}_2 \quad (8)$$

The vector component \bar{a} is set decrease from the value of 2 until 0. The \bar{r}_1 and \bar{r}_2 are random vectors with range [0,1]. The social hierarchy of grey wolves in hunting a prey can be depicted using a 3-dimensional prism as illustrated in Figure 4(a). Figure 4(b) depicts the updating position of respective wolves following the position of target prey.

3.2. Hunt the prey mechanism

In hunting, alpha wolves lead coordination with beta wolves and delta wolves. Assuming that the prey position is well known, the computation is achieved by obtaining the three best solutions namely alpha, beta and delta. Next, the delta agents need to update their positions to get the best search results. This hunting process is expressed in (9) and (10). The next position of the grey wolves is formulated in (11).

$$\bar{D}_\alpha = |\bar{C}_1 \cdot \bar{X}_\alpha - \bar{X}_g|; \bar{D}_\beta = |\bar{C}_2 \cdot \bar{X}_\beta - \bar{X}_g|; \bar{D}_\delta = |\bar{C}_3 \cdot \bar{X}_\delta - \bar{X}_g| \quad (9)$$

$$\bar{X}_1 = \bar{X}_\alpha - \bar{A}_1 \cdot \bar{D}_\alpha; \bar{X}_2 = \bar{X}_\beta - \bar{A}_2 \cdot \bar{D}_\beta; \bar{X}_3 = \bar{X}_\delta - \bar{A}_3 \cdot \bar{D}_\delta \quad (10)$$

$$\bar{X}_g(iter + 1) = \frac{1}{3} (\bar{X}_1 + \bar{X}_2 + \bar{X}_3) \quad (11)$$

3.3. Attacking the prey or search for the prey

The attack session is conducted when a target is tired, exhausted and finally stops at a certain point. When the position of wolves is less than 1 ($|A| < 1$), the predators are ready to force their prey. This situation is illustrated in Figure 5(a). The predators get new positions (to seek the new prey) in hunting process. In situation for the predators are spread out and the distance of respective predators is far away. Figure 5(b) illustrates search for the prey situation in this scheme. The complete explanation of hunting mechanism is given in [33].

The GWO for adjusting input-output parameters the inverter is built as: Population initialize, GWO parameters, and maximum generation (iteration, iter). For the current generation is less than max generation, the values of respective search agents are updated. The HVDC simulation is run on Simulink mode. The fitness of search agents are computed and evaluated in this session. Moreover, the position of search agents, best alpha score and their position are calculated. Ultimate, the score of best-alpha and their-position are printed, the program is ended. Figures 6(a) and 6(b) depict the algorithm and quasi-code computer program of GWO process.

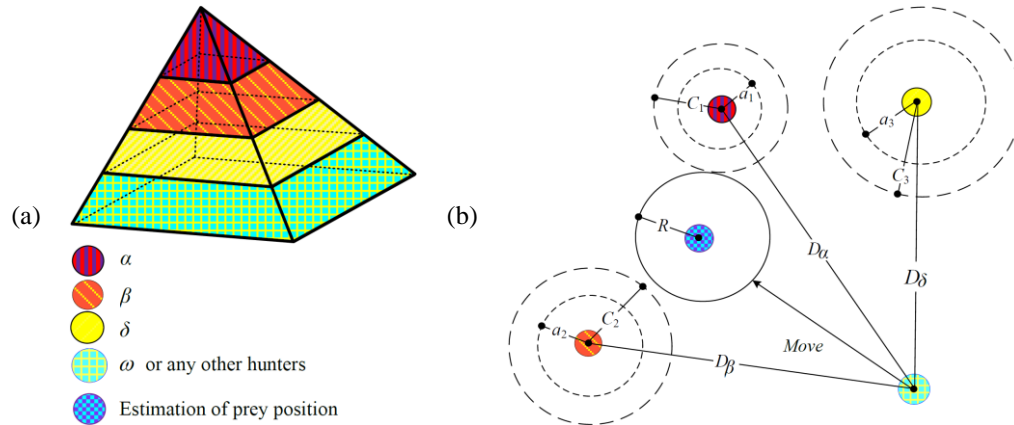


Figure 4. Diagram: (a) social hierarchy of grey wolf in hunting and (b) update position of respective grey wolves

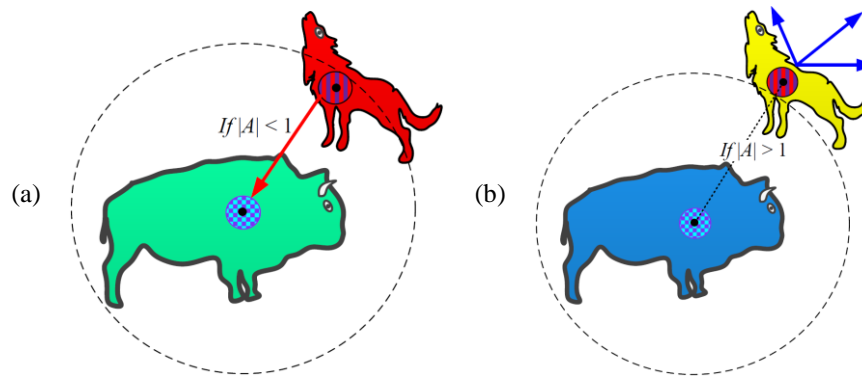
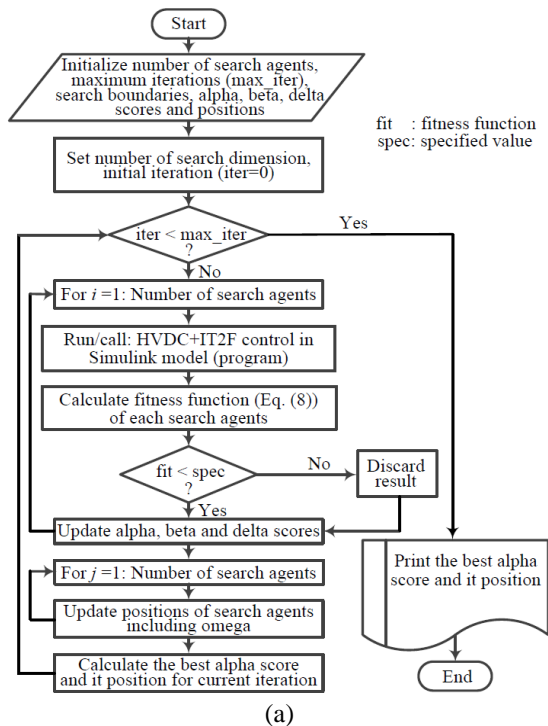


Figure 5. Decision mechanism on hunting session: (a) mode attacking and (b) mode searching



```

%Grey wolf optimizer (GWO) pseudo code for inverter transient response
%improvement in HVDC transmission link

Initialize the grey wolf population  $X_i$  ( $i=1, 2, \dots, n$ )

Initialize the  $\alpha$ ,  $A$  and  $C$ 

Calculate the fitness of each search agent

 $X_\alpha$  = the best search agent ( $X_{\alpha}$ )
 $X_\beta$  = the second search agent ( $X_{\beta}$ )
 $X_\delta$  = the third search agent ( $X_{\delta}$ )

while (iter < maximum number of iteration)
    for each search agent
        Update the position of current search agent by Eq. (7)
        Call HVDC equipped by IT2F-GWO control in Simulink model
    end for
    Update the  $\alpha$ ,  $A$  and  $C$ 
    Calculate the fitness function using Eq. (8) of all search agents
    Update the  $X_\alpha$ ,  $X_\beta$  and  $X_\delta$ 
    iter = iter + 1
end while

return  $X_\alpha$ 
  
```

(b)

Figure 6. GWO procedure to adjust the input-output parameters: (a) flow chart and (b) pseudo code for inverter

4. RESULTS AND DISCUSSION

In this section, validation of the HVDC system equipped by proposed control was simulated in time domain using MATLAB/Simulink model [34]. The simulation was tested on server computer Xeon E5-2673 V4, RAM 128 Gb, NVIDIA VGA GDDR 6 GB hardware. Integral time squared error (ITSE) and peak overshoot (M_p) criteria are used to assess the performance of the proposed controller. Start-up parameters are current reference (I_r) at 1.0; 1.1 pu; up-ramp time at 0.4 s; for Scenario A and Scenario B. The up-ramp rate parameters are increased from 20 to 35 pu/s. Simulation results are illustrated in Figures 7-11. The results also presented in Tables 1 and 2, respectively.

4.1. Parameter set-up of grey wolf optimizer (GWO)

In order to obtain the optimized regulation, the parameters of GWO were set: Search agent (Sa), number of variables, lower and upper of the variables, and maximum of iteration (max_iter). The Sa was at 5, 10, 15, 20, 25 and 30. The upper bound of variables were taken at [1 1 15], and lower bound of variables [.01 .01 .01], for K_{in1} , K_{in2} , and K_{out} , respectively. The max_iter was taken at 40 iterations. The convergence curve for up-ramp rate 35 pu/s, at time .4 s and final value at 1.1 pu, is shown Figure 7. It is shown that at the search agents: 5, the ITSE was slow to convergence at 24 iterations. By increasing the search agent, the convergence was achieved at less iteration. At the search agent 30, the convergence was occurred at 4 iterations.

Table 1. The ITSE performance of IT2FC on 3-phase inverter at current reference 1.0 pu

Up-ramp rate (Urr)	PI						IT2FC-GWO					
	I_a		I_b		I_c		I_a		I_b		I_c	
	ITSE ($\times 10^{-3}$)	M_p (%)	ITSE ($\times 10^{-3}$)	M_p (%)	ITSE ($\times 10^{-3}$)	M_p (%)	ITSE ($\times 10^{-3}$)	M_p (%)	ITSE ($\times 10^{-3}$)	M_p (%)	ITSE ($\times 10^{-3}$)	M_p (%)
20	1.6530	6.7493	1.6519	6.8955	1.6632	6.9361	1.5087	3.8223	1.5197	3.4334	1.5299	3.9740
21	1.7624	7.5800	1.7541	7.4958	1.7643	7.5782	1.5957	3.8377	1.5820	3.7444	1.5936	4.0005
22	1.8945	8.9901	1.8772	8.8262	1.8907	8.9626	1.6630	4.1772	1.5740	4.5865	1.6884	4.6317
23	1.9937	9.4446	1.9809	9.3677	1.9833	9.0551	1.7785	5.1644	1.7549	5.2720	1.7779	5.1220
24	2.1057	10.1371	2.0881	9.9849	2.0962	9.8414	1.8648	5.6598	1.8395	5.4171	1.8623	5.6758
25	2.2172	10.7015	2.2033	10.4952	2.1967	10.2317	1.9540	6.4347	1.9334	5.6434	1.9526	6.4192
26	2.3225	11.4338	2.3131	11.2719	2.3275	11.6193	2.0558	6.9433	2.0305	6.9513	2.0589	7.3300
27	2.4191	11.9613	2.3979	11.6439	2.4194	12.2321	2.1325	7.4476	2.1196	7.3639	2.1349	7.4494
28	2.5123	12.5904	2.4963	12.4343	2.5022	12.2481	2.2324	8.0147	2.1937	8.0528	2.2070	7.7225
29	2.6281	13.1373	2.5967	13.2094	2.6162	13.0176	2.3343	8.5540	2.3023	8.6216	2.2916	8.4816
30	2.7302	13.8254	2.6989	13.9991	2.7028	13.5392	2.3809	8.6259	2.3588	8.5946	2.3698	8.4804
31	2.8278	14.1791	2.8117	14.3544	2.8047	13.9216	2.4632	9.0952	2.4635	9.0627	2.4503	8.7689
32	2.8949	14.2968	2.8951	14.7650	2.8713	14.3631	2.5507	9.4354	2.5382	9.3960	2.5273	9.1091
33	2.9819	14.6557	2.9781	15.1542	2.9697	14.8381	2.5930	9.3214	2.5803	9.3968	2.5817	9.1867
34	3.0861	15.6414	3.0731	15.4896	3.0771	15.7989	2.6488	9.8639	2.6457	9.6666	2.6477	9.5550
35	3.1789	16.0709	3.1748	15.9423	3.1579	16.2342	2.7204	9.9827	2.7088	9.8966	2.7038	9.5511

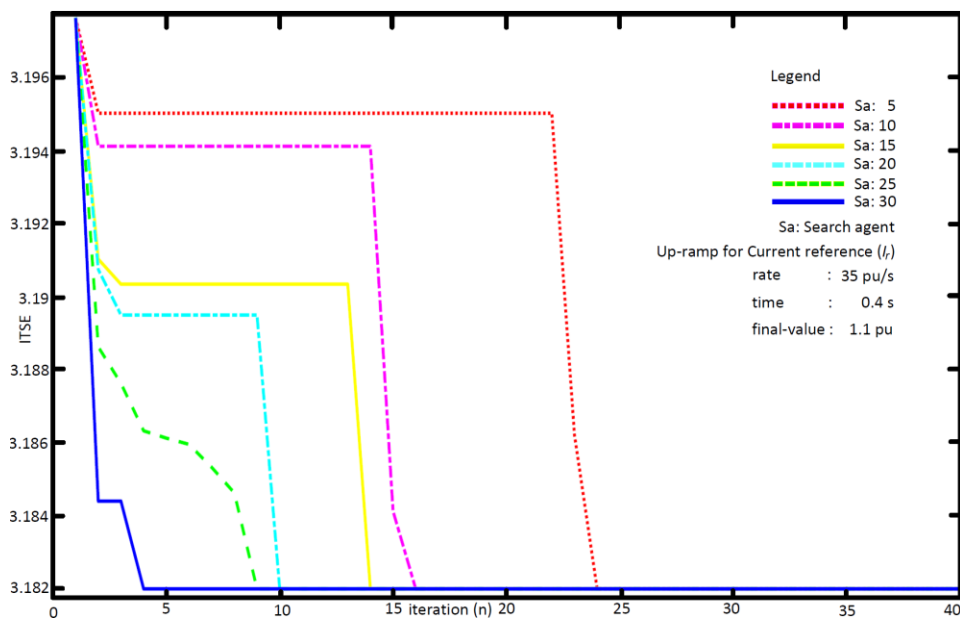


Figure 7. GWO convergence curve for running in 40 iterations

4.2. Scenario A

In this scenario, IT2FC is applied to control the HVDC system, and this system was evaluated on transient response in time domain simulation. Figure 8 shows time domain of inverter transient responses of the IT2FC compared to the PI controller for current reference (I_r) at 1.0 pu and first step *Up-ramp rate* (Urr) 20 pu/s at starting time. The ITSE of PI controller was obtained at $(1.6530; 1.6519 \text{ and } 1.6632) \times 10^{-3}$, for phase A, B and C, respectively. Peak overshoot occurred at 6.7493; 6.8955 and 6.9361 % for phase A, B and C, of PI controller. Next step, the Urr was increased to 21 pu/s, the ITSE increased also to $(1.7624; 1.7541 \text{ and } 1.7643) \times 10^{-3}$, for phase A, B and C. When the Urr was increased again to 22 pu/s, the ITSE achieved at $(1.8945; 1.8772 \text{ and } 1.8907) \times 10^{-3}$, for phase A, B and C. Final step, the Urr at 35 pu/s, so the ITSE was obtained at $(3.1789; 3.1748 \text{ and } 3.1579) \times 10^{-3}$, for phase A, B and C, respectively. Peak overshoot in this scheme occurred at 15.6414; 15.4896 and 15.7989 % for phase A, B and C, of PI controller.

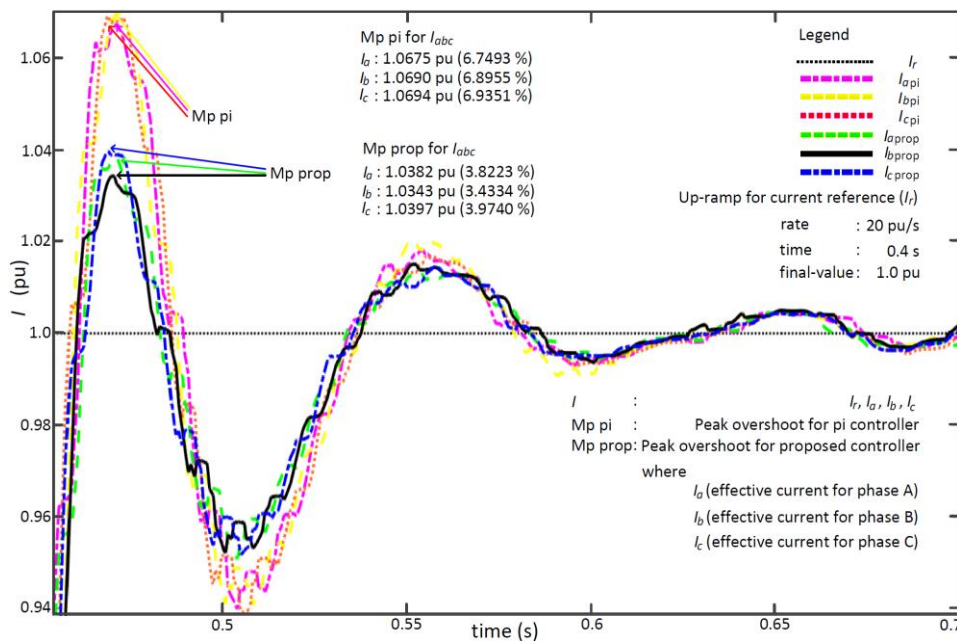


Figure 8. Improvement of inverter transient response for up-ramp rate at 20 pu/s

When the IT2FC was setup at the Urr 20 pu/s, the ITSE obtained at $(1.5087; 1.5197 \text{ and } 1.5299) \times 10^{-3}$, for phase A, B and C. While, peak overshoot was at 3.8223; 3.4334 and 3.974 % for phase A, B and C, of proposed controller. For the Urr was increased to 21 pu/s, the ITSE achieved at $(1.5957; 1.582 \text{ and } 1.5936) \times 10^{-3}$, for phase A, B and C. For up-ramp rate increased again at 22 pu/s, the ITSE was at $(1.663; 1.574 \text{ and } 1.6884) \times 10^{-3}$, for phase A, B and C. For final step, the Urr at 35 pu/s, the ITSE was obtained at $(2.7204; 2.7088 \text{ and } 2.7038) \times 10^{-3}$, for phase A, B and C, respectively. The peak overshoot for this scheme was at 9.8639; 9.6666 and 9.555 % for phase A, B and C, of proposed controller. The improvement of inverter transient response of proposed controller for the Urr 35 pu/s is illustrated in Figure 9. Based on the simulation results in the Scenario A, it is shown that the proposed controller gives smaller ITSE and peak overshoot values than the PI controller.

4.3. Scenario B

Next simulation, the proposed controller was tested on the current reference at 1.1 pu and Urr increased from 20 until 35 pu/s, and listed in Table 2. Figure 10 shows the inverter transient response of proposed controller compared to PI controller. Simulation results of the HVDC under these conditions are listed in Table 2.

In first step, the Urr at 20 pu/s, the ITSE value was at $(1.8195; 1.8098 \text{ and } 1.8245) \times 10^{-3}$, for phase A, B and C, of PI controller. Peak overshoot (Mp) was obtained at 4.9507; 4.9441 and 4.8078 % for phase A, B and C, respectively. The Urr was increased to 21 pu/s in next step, the ITSE achieved at $(1.9483; 1.9399 \text{ and } 1.9478) \times 10^{-3}$, for phase A, B and C. For final step at the Urr 35 pu/s, so the ITSE was obtained at $(3.699; 3.6953 \text{ and } 3.6574) \times 10^{-3}$, for phase A, B and C, respectively. The Mp was obtained at 12.7642; 12.7896 and 12.7747 % for phase A, B and C.

Meanwhile, the IT2FC was tested on the U_{rr} at 20 pu/s, ITSE performance was obtained at $(1.6855; 1.692 \text{ and } 1.7039) \times 10^{-3}$ for phase A, B and C. Peak overshoot was at 2.4247; 2.3295 and 2.1824 % for phase A, B and C. Next, the U_{rr} was increased to 21 pu/s and the ITSE was obtained at $(1.7813; 1.7815 \text{ and } 1.7709) \times 10^{-3}$, for phase A, B and C. Finally, when the U_{rr} was increased into 35 pu/s the ITSE achieved at $(3.2076; 3.1789 \text{ and } 3.1691) \times 10^{-3}$, for phase A, B and C. The peak overshoot for this session was at 9.2791; 9.238 and 9.0031 % for phase A, B and C, respectively. The transient response maintain for up-ramp rate 35 pu/s is shown in Figure 11. Based on the simulation results, it is shown that the proposed controller gives smaller ITSE and M_p values than the PI controller.

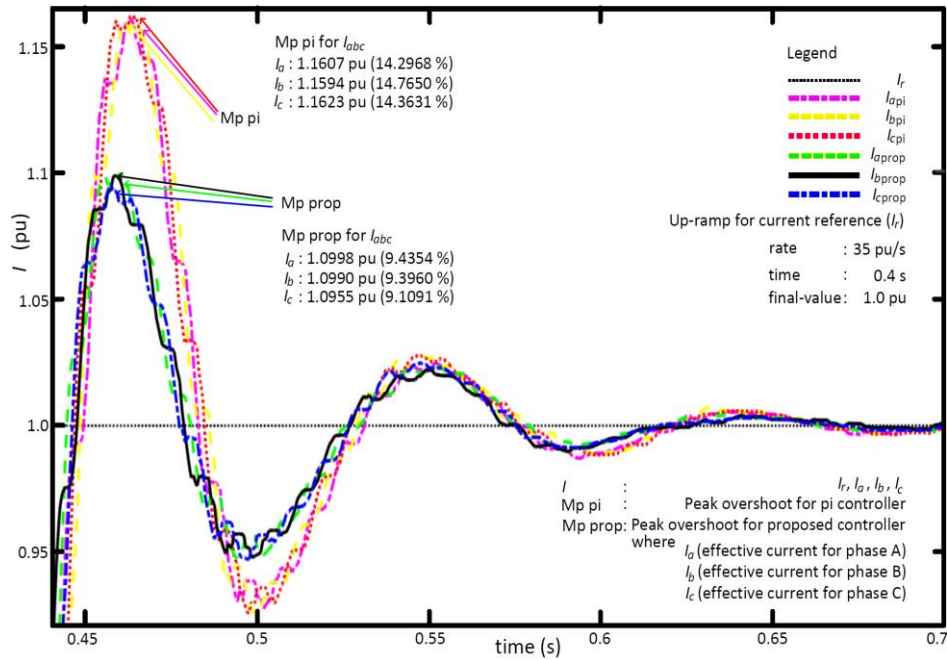


Figure 9. Inverter transient response at up-ramp rate 35 pu/s

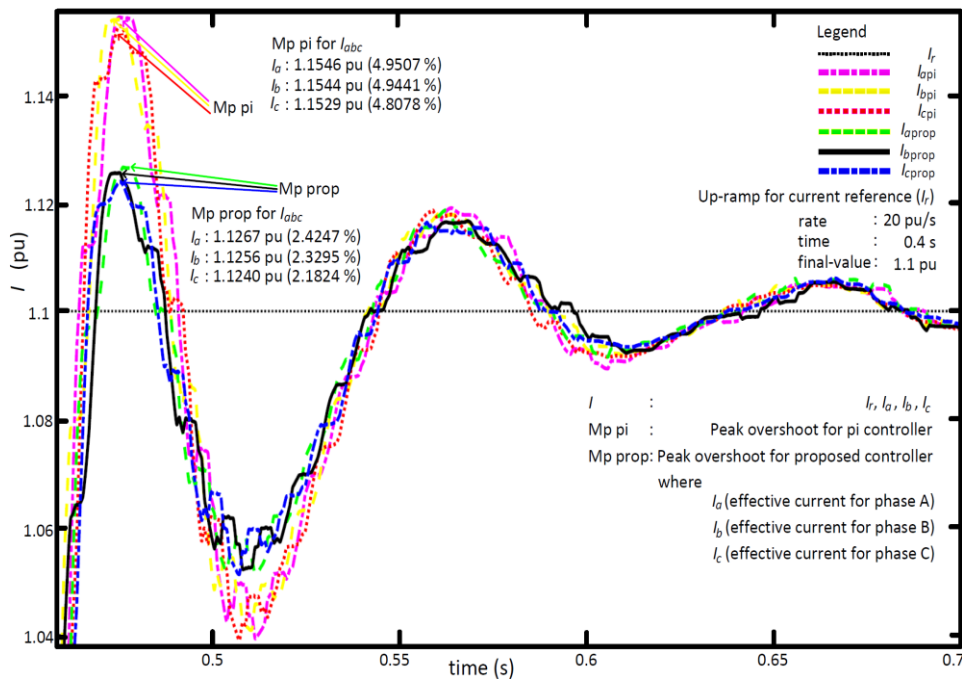


Figure 10. Comparison responses of proposed control and PI control

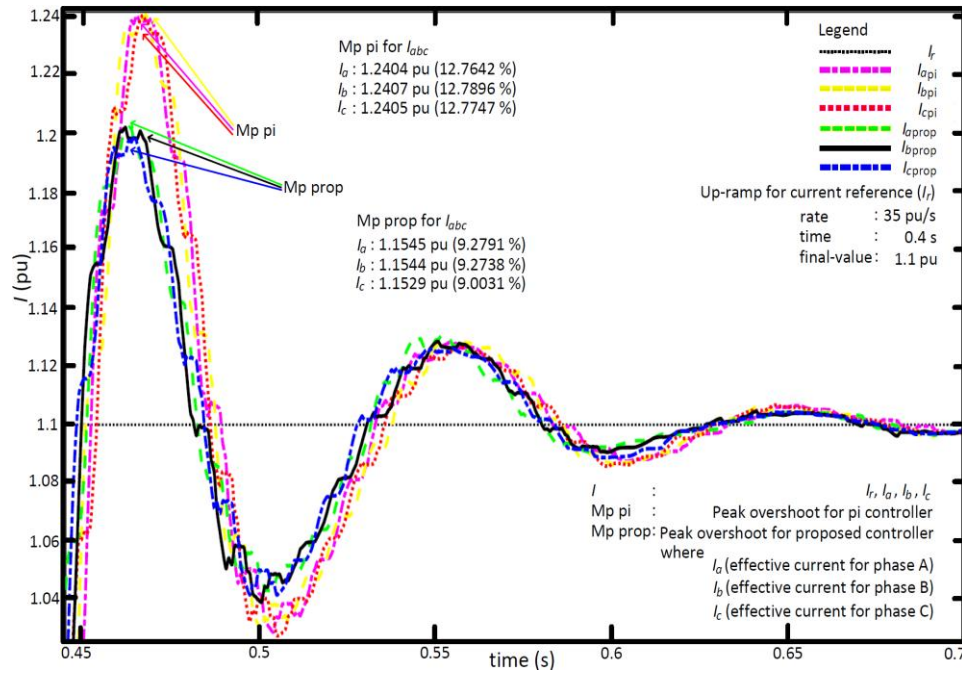


Figure 11. Maintain of inverter transient response for up-ramp rate 35 pu/s

Table 2. The proposed control performance for 3-phase inverter at the I_r increased to 1.1 pu

Up-ramp rate (Urr)	PI				IT2FC-GWO							
	I_a	M_p	I_b	M_p	I_c	M_p	I_a	M_p	I_b	M_p	I_c	M_p
	ITSE ($\times 10^{-3}$)	(%)	ITSE ($\times 10^{-3}$)	(%)	ITSE ($\times 10^{-3}$)	(%)	ITSE ($\times 10^{-3}$)	(%)	ITSE ($\times 10^{-3}$)	(%)	ITSE ($\times 10^{-3}$)	(%)
20	1.8195	4.9507	1.8098	4.9441	1.8245	4.8078	1.6855	2.4247	1.6920	2.3295	1.7039	2.1824
21	1.9483	6.0565	1.9399	6.0452	1.9478	5.5257	1.7813	2.6562	1.7815	2.6795	1.7709	2.5011
22	2.0854	6.6872	2.0755	6.7594	2.0929	6.7097	1.8582	2.9209	1.8619	2.7319	1.8878	3.3055
23	2.2204	7.4901	2.2057	8.0743	2.2158	7.9319	1.9783	3.4170	1.9630	3.7681	1.9857	3.8819
24	2.3659	8.6675	2.3437	8.6607	2.3487	8.7292	2.0834	4.0639	2.0586	4.2018	2.0765	4.0568
25	2.5029	9.2453	2.4828	9.0527	2.4803	9.4746	2.1954	4.7741	2.1698	4.6786	2.1910	4.6035
26	2.6359	9.9316	2.6305	9.8897	2.6253	10.1042	2.2938	5.0132	2.2773	5.2955	2.2788	5.0155
27	2.7614	10.6365	2.7543	10.3787	2.7554	10.7459	2.4032	5.5476	2.3844	5.6899	2.3973	5.0569
28	2.8841	11.0524	2.8803	11.0869	2.8834	11.6026	2.5207	6.3081	2.4963	6.1299	2.4961	6.6181
29	3.0537	12.4717	3.0352	12.3454	3.0492	12.7266	2.6142	6.9581	2.5925	6.8780	2.6089	6.9315
30	3.1769	12.9699	3.1607	12.9352	3.1712	13.1374	2.6998	7.3331	2.7008	7.2610	2.7252	7.6621
31	3.2811	12.8165	3.2630	12.7754	3.2634	12.8823	2.8455	8.0133	2.8226	7.9602	2.8222	7.9808
32	3.3765	12.8980	3.3623	12.6960	3.3442	12.7578	2.9311	8.1559	2.8994	8.3103	2.9222	8.2644
33	3.4889	12.9394	3.4757	12.8978	3.4635	12.8369	3.0085	8.4860	2.9887	8.6829	3.0000	8.5307
34	3.5938	12.7596	3.5774	12.8264	3.5597	12.8149	3.0893	8.5918	3.0695	8.7278	3.0753	8.7533
35	3.6990	12.7642	3.6953	12.7896	3.6574	12.7747	3.2076	9.2791	3.1789	9.2738	3.1691	9.0031

5. CONCLUSION

In this research the GWO algorithm applied to adjust the input-output parameter of IT2FC is provided on inverter HVDC-link system to improve transient response at start-up period time. The IT2FC is developed by two inputs and an output model. Five Gaussian type membership functions (MFs) are used to map the crisp value on the respective inputs to the fuzzy value. Nine constant type MFs are implemented to map the fuzzy rules based to crisp value of output. The ITSE scheme is implemented to assess the transient response of the inverter HVDC. Scenario A: When the up-ramp rate (Urr) is given at 20 pu/s, the ITSE achieved at $(1.6530; 1.6519 \text{ and } 1.6632) \times 10^{-3}$, for phase A, B, and C, of PI controller, respectively. Peak overshoot occurred at 6.7493; 6.8955 and 6.9361 % for phase A, B, and C. When the Urr at 35 pu/s, the ITSE obtained at $(1.6530; 1.6519 \text{ and } 1.6632) \times 10^{-3}$, for phase A, B and C. Peak overshoot (M_p) achieved at 6.7493; 6.8955 and 6.9361 % for phase A, B and C. Scenario B: For the Urr is given at 20 pu/s, the ITSE obtained at $(1.8195; 1.8098 \text{ and } 1.8245) \times 10^{-3}$, for phase A, B and C, for PI controller. The M_p is 4.9507; 4.9441 and 4.8078 % for phase A, B and C. For the Urr increased to 35 pu/s, the ITSE is $(3.2076; 3.1789 \text{ and } 3.1691) \times 10^{-3}$, for phase A, B and C. The M_p obtained at 9.2791; 0.238 and 9.0031 % for respective phase A,

B and C. The IT2FC gives better results with smaller ITSE values for Scenarios A and B compared to PI controller. Also the M_p of the IT2FC is lower than the M_p of the traditional PI for all scenarios.

ACKNOWLEDGMENTS

The authors thank to the directorate general of higher education (DGHE) of Indonesia Republic for all financial support through “Penelitian Fundamental-Reguler 2024” research scheme.

FUNDING INFORMATION

This research was founded by the National Research Grand of Indonesia “Penelitian Fundamental-Reguler Tahun Anggaran 2024” research scheme under contract number: 3019/UN18.L1/PP/2024.

AUTHOR CONTRIBUTIONS STATEMENT

This journal uses the Contributor Roles Taxonomy (CRediT) to recognize individual author contributions, reduce authorship disputes, and facilitate collaboration.

Name of Author	C	M	So	Va	Fo	I	R	D	O	E	Vi	Su	P	Fu
I Made Ginarsa	✓	✓	✓	✓	✓	✓		✓	✓	✓			✓	
Agung Budi Muljono		✓				✓		✓	✓	✓	✓	✓		
I Made Ari Nnartha	✓		✓	✓			✓			✓	✓		✓	
Ni Made Seniari	✓				✓			✓		✓	✓			
Sultan		✓			✓		✓			✓		✓		
Osea Zebua	✓	✓	✓	✓		✓		✓	✓		✓		✓	

C : Conceptualization	I : Investigation	Vi : Visualization
M : Methodology	R : Resources	Su : Supervision
So : Software	D : Data Curation	P : Project administration
Va : Validation	O : Writing - Original Draft	Fu : Funding acquisition
Fo : Formal analysis	E : Writing - Review & Editing	

CONFLICT OF INTEREST STATEMENT

The authors state no conflict of interest.

DATA AVAILABILITY

The authors confirm that the data supporting the findings of this study are available in [31].

REFERENCES

[1] T. Lu, H. Feng, Z. Zhao, and X. Cui, “Analysis of the electric field and ion current density under ultra high-voltage direct-current transmission lines based on finite element method,” *IEEE Transactions on Magnetics*, vol. 43, no. 4, pp. 1221–1224, 2007, doi: 10.1109/TMAG.2006.890960.

[2] Y. Liu, L. Zhou, H. Yuan, Y. Liu, and L. Ji, “Analysis of self-correlation characteristics of corona current spectrum on UHVDC transmission line,” *IEEE Transactions on Dielectrics and Electrical Insulation*, vol. 25, no. 3, pp. 928–938, Jun. 2018, doi: 10.1109/TDEI.2018.006933.

[3] S. Chen, S. Lin, Y. Yang, K. Jiang, and M. Liu, “Assessment and enhancement of transfer capability for large-scale renewable generation base transmitted by voltage source converter based high voltage direct current system,” *International Journal of Electrical Power & Energy Systems*, vol. 165, p. 110506, Apr. 2025, doi: 10.1016/j.ijepes.2025.110506.

[4] Daochun Huang, Yinbiao Shu, Jiangjun Ruan, and Yi Hu, “Ultra high voltage transmission in china: developments, current status and future prospects,” *Proceedings of the IEEE*, vol. 97, no. 3, pp. 555–583, Mar. 2009, doi: 10.1109/JPROC.2009.2013613.

[5] Kaigui Xie, Bo Hu, and C. Singh, “Reliability evaluation of double 12-pulse ultra HVDC transmission systems,” *IEEE Transactions on Power Delivery*, vol. 31, no. 1, pp. 210–218, Feb. 2016, doi: 10.1109/TPWRD.2015.2489658.

[6] M. Rosyadi *et al.*, “A simplified model design of MMC-HVDC transmission system for steady state and transient stability analyses,” *International Journal of Power Electronics and Drive Systems (IJPEDS)*, vol. 14, no. 2, p. 934, Jun. 2023, doi: 10.11591/ijpeds.v14.i2.pp934-947.

[7] H. Xiao, Z. Xu, L. Xiao, C. Gan, F. Xu, and L. Dai, “Components sharing based integrated HVDC circuit breaker for meshed HVDC Grids,” *IEEE Transactions on Power Delivery*, vol. 35, no. 4, pp. 1856–1866, Aug. 2020, doi: 10.1109/TPWRD.2019.2955726.




[8] H. Zhang, K. Wei, Y. Wei, and H. Zhu, “Emergency power control strategy of HVDC FLC based on modified SFR model in islanded HVDC sending system,” *International Journal of Electrical Power and Energy Systems*, vol. 142, p. 108314, Nov. 2022, doi: 10.1016/j.ijepes.2022.108314.

[9] D.-H. Kwon, Y.-J. Kim, and O. Gomis-Bellmunt, “Optimal DC voltage and current control of an LCC HVDC system to improve real-time frequency regulation in rectifier- and inverter-side grids,” *IEEE Transactions on Power Systems*, vol. 35, no. 6, pp. 4539–4553, Nov. 2020, doi: 10.1109/TPWRS.2020.2997793.





- [10] D.-H. Kwon and Y.-J. Kim, "Optimal data-driven control of an LCC HVDC system for real-time grid frequency regulation," *IEEE Access*, vol. 8, pp. 58470–58482, 2020, doi: 10.1109/ACCESS.2020.2981598.
- [11] B. Ren, Y. Luo, N. Zhou, and Q. Wang, "Fault location in high-voltage direct-current grids based on panoramic voltage features and vision transformers," *International Journal of Electrical Power & Energy Systems*, vol. 158, p. 109958, Jul. 2024, doi: 10.1016/j.ijepes.2024.109958.
- [12] S. Asvapoositkul and R. Preece, "Impact of HVDC dynamic modelling on power system small signal stability assessment," *International Journal of Electrical Power & Energy Systems*, vol. 123, p. 106327, Dec. 2020, doi: 10.1016/j.ijepes.2020.106327.
- [13] X. Chen, Y. Liang, G. Wang, H. Li, B. Li, and Z. Guo, "A control parameter analysis method based on a transfer function matrix of hybrid multi-terminal HVDC system with flexible adaptability for different operation modes," *International Journal of Electrical Power & Energy Systems*, vol. 116, p. 105584, Mar. 2020, doi: 10.1016/j.ijepes.2019.105584.
- [14] J. Serrano-Sillero and M. Á. Moreno, "Small-signal stability analysis of the asymmetrical DC operation in HVDC networks," *Electric Power Systems Research*, vol. 214, p. 108942, Jan. 2023, doi: 10.1016/j.epr.2022.108942.
- [15] M. Romero-Rodríguez, R. Delpoux, L. Piétrac, J. Dai, A. Benchaib, and E. Niel, "An implementation method for the supervisory control of time-driven systems applied to high-voltage direct current transmission grids," *Control Engineering Practice*, vol. 82, pp. 97–107, Jan. 2019, doi: 10.1016/j.conengprac.2018.10.002.
- [16] M. Aragüés-Peñalba, J. Sau Bassols, S. Galceran Arellano, A. Sumper, and O. Gomis Bellmunt, "Optimal operation of hybrid high voltage direct current and alternating current networks based on OPF combined with droop voltage control," *International Journal of Electrical Power & Energy Systems*, vol. 101, pp. 176–188, Oct. 2018, doi: 10.1016/j.ijepes.2018.03.010.
- [17] J.-S. Lim, D.-H. Kwon, Y.-T. Yoon, and S.-I. Moon, "Optimal control scheme for multi-terminal high-voltage direct current system to improve robust grid frequency regulations," *Energy Reports*, vol. 12, pp. 529–543, Dec. 2024, doi: 10.1016/j.egyr.2024.06.005.
- [18] C. Guo, S. Member, W. Zhao, S. Yang, Z. Wu, and C. Zhao, "Current balancing control approach for paralleled MMC groups in hybrid LCC / VSC cascaded HVDC system," 2022.
- [19] D. Zhang, C. Wu, P. Ni, and J. He, "Double-ended fast protection system of LCC-VSC-MTDC independent on boundary component," *CSEE Journal of Power and Energy Systems*, 2022, doi: 10.17775/CSEEJPES.2021.05810.
- [20] M. Mehra, M. Babaie, A. Zafari, and K. Al-Haddad, "Passivity ANFIS-based control for an intelligent compact multilevel converter," *IEEE Transactions on Industrial Informatics*, vol. 17, no. 8, pp. 5141–5151, Aug. 2021, doi: 10.1109/TII.2021.3049313.
- [21] I. M. Ginarsa, A. B. Muljono, I. M. A. Nrartha, and S. Sultan, "Transient response improvement of direct current using supplementary control based on ANFIS for rectifier in HVDC," *International Journal of Power Electronics and Drive Systems (IJPEDS)*, vol. 11, no. 4, p. 2107, Dec. 2020, doi: 10.11591/ijpeds.v11.i4.pp2107-2115.
- [22] I. M. Ginarsa, I. M. A. Nrartha, A. B. Muljono, S. Sultan, N. M. Seniari, and I. M. B. Sukmadana, "Transient current maintenance using controller based on recurrent neural network in high voltage direct current approximation model," in *2023 International Conference on Smart-Green Technology in Electrical and Information Systems (ICSGTEIS)*, IEEE, Nov. 2023, pp. 178–183. doi: 10.1109/ICSGTEIS60500.2023.10424319.
- [23] A. Cheraghali, M. Hajiaghahi-Kesheli, and M. M. Paydar, "Tree growth algorithm (TGA): a novel approach for solving optimization problems," *Engineering Applications of Artificial Intelligence*, vol. 72, pp. 393–414, Jun. 2018, doi: 10.1016/j.engappai.2018.04.021.
- [24] H. T. Sadeeq and A. M. Abdulazeez, "Giant trevally optimizer (GTO): a novel metaheuristic algorithm for global optimization and challenging engineering problems," *IEEE Access*, vol. 10, pp. 121615–121640, 2022, doi: 10.1109/ACCESS.2022.3223388.
- [25] S. Yadav, H. R. Chamorro, W. C. Flores, and R. K. Mehta, "Investigation of improved thermal dissipation of ±800 kV converter transformer bushing employing nano-hexagonal boron nitride paper using FEM," *IEEE Access*, vol. 9, pp. 149196–149217, 2021, doi: 10.1109/ACCESS.2021.3124917.
- [26] P. Trojovský, "A new human-based metaheuristic algorithm for solving optimization problems based on preschool education," *Scientific Reports*, vol. 13, no. 1, p. 21472, Dec. 2023, doi: 10.1038/s41598-023-48462-1.
- [27] M. Najafi Ashtiani, A. Toopshekan, F. Razi Astarai, H. Yousefi, and A. Maleki, "Techno-economic analysis of a grid-connected PV/battery system using the teaching-learning-based optimization algorithm," *Solar Energy*, vol. 203, pp. 69–82, Jun. 2020, doi: 10.1016/j.solener.2020.04.007.
- [28] S. Talatahari, M. Azizi, M. Tolouei, B. Talatahari, and P. Sareh, "Crystal structure algorithm (CryStAl): a metaheuristic optimization method," *IEEE Access*, vol. 9, pp. 71244–71261, 2021, doi: 10.1109/ACCESS.2021.3079161.
- [29] B. Nouhi, N. Khodadadi, M. Azizi, S. Talatahari, and A. H. Gandomi, "Multi-objective material generation algorithm (MOMGA) for optimization purposes," *IEEE Access*, vol. 10, pp. 107095–107115, 2022, doi: 10.1109/ACCESS.2022.3211529.
- [30] V. Veerasamy *et al.*, "A hankel matrix based reduced order model for stability analysis of hybrid power system using PSO-GSA optimized cascade PI-PD controller for automatic load frequency control," *IEEE Access*, vol. 8, pp. 71422–71446, 2020, doi: 10.1109/ACCESS.2020.2987387.
- [31] S. Casario, "Thyristor-based HVDC transmission system," *Hydro-Quebec*, 2013.
- [32] K. M. Sreedivya, P. Aruna Jeyanthi, and D. Devaraj, "Improved design of interval type-2 fuzzy based wide area power system stabilizer for inter-area oscillation damping," *Microprocessors and Microsystems*, vol. 83, p. 103957, Jun. 2021, doi: 10.1016/j.micpro.2021.103957.
- [33] S. Mirjalili, S. M. Mirjalili, and A. Lewis, "Grey wolf optimizer," *Advances in Engineering Software*, vol. 69, pp. 46–61, Mar. 2014, doi: 10.1016/j.advengsoft.2013.12.007.
- [34] MATLAB, "MATLAB Simulink R2022a," *The MathWorks, Inc*, 2022.

BIOGRAPHIES OF AUTHORS







I Made Ginarsa    is a lecturer in the Electrical Engineering Department received the B.Eng. (1997), M.T. (2001), and Ph.D. (2012) degrees in electrical engineering from Udayana, Gadjah Mada Universities, and Institut Teknologi Sepuluh Nopember, Indonesia, respectively. He is a lecturer at the Department of Electrical Engineering, University of Mataram. In 2010, he was a member of the EPS Laboratory, Kumamoto University. His research is on voltage and dynamic stability, nonlinear dynamics, application of artificial intelligence in high voltage direct current and power systems. He was a member of the Institution of Engineers Indonesia, an author, co-author, and invited reviewer on national and international publications. He can be contacted at email: kadekgin@unram.ac.id.







Agung Budi Muljono     is a lecturer in the Electrical and Electronic Engineering Department. He received the B.Eng. and M.Eng. in Electrical Engineering from Malang Institute of Technology (1996) and UGM (2000), respectively. He is a member of IEEE, FORTEL, and the Institution of Engineers Indonesia. He has authored and co-authored several papers and serves on the editorial board of the Dielektrika Journal. His research interests include transmission and distribution, dynamic and stability, artificial intelligence applications, and energy planning and distributed generation in power systems. He can be contacted at email: agungbm@unram.ac.id.







I Made Ari Nrartha     received in B.Eng. and M.Eng. in electrical engineering from the Institute Technology Sepuluh Nopember, Surabaya, and Gadjah Mada University, Yogyakarta, Indonesia, in 1997 and 2001, respectively. Since 1999, he has been a lecturer in electrical engineering at the University of Mataram. His research interests are power system dynamics and stability, transmission and distribution, optimization, power quality, and artificial intelligence applications in power systems. He was a member of the Institution of Engineers Indonesia, an active author and co-author of research papers in national and international journals, and served as the editorial board of Dielektrika Journal. He can be contacted at email: nrartha@unram.ac.id.







Ni Made Seniari     is a lecturer in the Electrical Engineering Department, University of Mataram, since 1997. She took her Bachelor of Engineering (1996) at the Department of Electrical Engineering, Udayana University, Bali, and her M. Eng. (2003) at Bandung Institute of Technology. Her research interests are power system electric, electric field, magnetic field, and induction voltage due to thunderstorm strike, and determining the safe zone of Base Transceiver System towers in residential areas. He was a member of the Institution of Engineers Indonesia, an author, and a co-author on national and international publications. She can be contacted at email: seniari_nimade@unram.ac.id.



Sultan     was born in Bulukumba, South Sulawesi, Indonesia. He received the B. Eng. and M.Eng. degrees in electrical engineering from Hassanudin University (1995) and UGM (2005), respectively. In 1997, he was a lecturer at the University of Mataram, Indonesia. His research interests include power system transmission and distribution, power system dynamics, and stability in power systems. He was an active author and co-author of research papers in national and international journals, and served as editor-in-chief of Dielektrika journal from 2010-2018. He can be contacted at email: sultandarma@unram.ac.id.



Osea Zebua     is a lecturer in the Electrical and Electronic Engineering Department at the University of Lampung, Indonesia, since 2001. He received the B.Eng. (1997) and M.Eng. (2001) degrees in electrical engineering from Sumatera Utara University and Gadjah Mada University, Indonesia, respectively. His research interests include power system operation, transmission and distribution, optimization, power quality, and artificial intelligence applications in power systems. He was an active author and co-author of research papers in national and international journals. He can be contacted at email: osea.zebua@eng.unila.ac.id.